

Selected-Control Synthesis of Metal Phosphonate Nanoparticles and Nanorods

Shu-Yan Song, Jian-Fang Ma,* Jin Yang, Min-Hua Cao, and Ke-Chun Li

Department of Chemistry, Northeast Normal University, Changchun 130024, P. R. China

Received November 7, 2004

By surfactant-assisted methods, nanoscale $\text{Co}(\text{O}_3\text{PC}_6\text{H}_5)\cdot\text{H}_2\text{O}$ species of different morphologies, namely, nanoparticles and nanorods, have been successfully synthesized and characterized. Upon removal of the organic part of the compound, peculiar $\text{Co}_2\text{P}_2\text{O}_7$ porous nanorods formed.

Nanometer-scale materials have attracted intensive attention in the past decades because of their unique physical and chemical properties and potential applications in nanodevices and functional materials.¹ Great progress has been made in the fabrication of inorganic and organic nanosize materials, such as carbon nanotubes, metal nanorods, metal oxides nanowires, and polyaniline nanoparticles.^{2–5} However, to the best of our knowledge, few reports on the synthesis of nanoscale metal phosphonates have been published to date.⁶ Owing to their specific characteristics and potential applications as sorbents, sensors, catalysts, ion exchangers, ionic conductors, and nonlinear optical materials,⁷ exploring proper

methods for the synthesis of nanoscale metal phosphonate proves to be intriguing and valuable.

Surfactant-assisted methods have been widely used in the preparation and morphology control of materials such as silica particles, silica nanotubes, carbon nanotubes, and CdS and CdSe nanorods.⁸ The surfactant plays an important role in determining the morphology of the products, as surfactant mesophases have proved to be useful and versatile soft templates that can form different conformations by self-assembly and lead to the formation of different nanostructures.⁹ Herein, we report a successful method using surfactants, namely, cetyltrimethylammonium bromide (CTAB) and sodium dodecyl benzene sulfonate (SDBS), for the preparation of $\text{Co}(\text{O}_3\text{PC}_6\text{H}_5)\cdot\text{H}_2\text{O}$ nanoparticles and nanorods under different conditions.

$\text{Co}(\text{O}_3\text{PC}_6\text{H}_5)\cdot\text{H}_2\text{O}$, which exhibits peculiar and fascinating magnetic properties including magnetic ordering, canted antiferromagnetism, and antiferromagnetic resonance, has been studied as a model for two-dimensional (2D) magnetism.¹⁰ The properties of inorganic and organic hybrid materials, such as catalytic activity, sensitivity, conductivity, and photonic efficiency, are often closely related to their chemical composition, size, crystal structure, surface chemistry, and shape.¹¹ Nanorods and nanoparticles often offer larger surface areas than the corresponding solid films or bulk materials. The ability to synthetically tune these material parameters, especially their size and morphology, then proves

* To whom correspondence should be addressed. E-mail: jfma@public.cc.jl.cn.

- (1) (a) Thurn-Albrecht, T.; Schotter, J.; Kastle, G. A.; Emley, N.; Shibauchi, T.; Krusin-Elbaum, L.; Guarini, K.; Black, C. T.; Tuominen, M. T.; Russell, T. P. *Science* **2000**, *290*, 2126. (b) Nicewarner-Pena, S. R.; Griffith Freeman, R.; Reiss, B. D.; He, L. Pena, D. J.; Walton, I. D.; Cromer, R.; Keating, C. D.; Natan, M. J. *Science* **2001**, *294*, 137. (c) Lu, L.; Wohlfart, A.; Parala, H.; Birkner, A.; Fischer, R. A. *Chem. Commun.* **2003**, *40*. (d) Xia, Y. N.; Yang, P. D.; Sun, Y.; Wu, Y.; Mayers, B.; Gates, B.; Yin, Y.; Kim, F.; Yan, H. *Adv. Mater.* **2003**, *15*, 353. (e) Rao, C. N. R.; Satishkumar, B. C.; Govindaraj, A. *Chem. Commun.* **1997**, 1581.
- (2) (a) Iijima, S. *Nature* **1991**, *56*, 354. (b) Trasobares, S.; Ewels, C. P.; Birrell, J.; Stephan, O.; Wei, B. Q.; Carlisle, J. A.; Miller, D.; Koblinski, P.; Ajayan, P. M. *Adv. Mater.* **2004**, *16*, 610.
- (3) (a) Liu, Z.; Bando, Y. *Adv. Mater.* **2003**, *15*, 303. (b) Chang, S.; Yoon, S.; Park, H.; Sakai, A. *Mater. Lett.* **2001**, *53*, 432. (c) Ah, C. S.; Hong, S. D.; Jang, D.-J. *J. Phys. Chem. B* **2001**, *105*, 7871.
- (4) (a) Rao, C. N. R.; Deepak, F. L.; Gundiah, G.; Govindaraj, A. *Prog. Solid State Chem.* **2003**, *31*, 5. (b) Li, C.; Zhang, D.; Han, S.; Liu, X.; Tang, T.; Zhou, C. *Adv. Mater.* **2003**, *15*, 143. (c) Huang, M.; Mao, S.; Feick, H.; Yan, H.; Wu, Y.; Kind, H.; Weber, E.; Russo, R.; Yang, P. *Science* **2001**, *292*, 1897. (d) Dai, Z. R.; Gole, J. L.; Stout, J. D.; Wang, Z. L. *J. Phys. Chem. B* **2002**, *106*, 1274. (e) Jiang, X.; Herricks, T.; Xia, Y. *Nano Lett.* **2002**, *2*, 1333.
- (5) (a) Kim, B.-J.; Oh, S.-G.; Han, M.-G.; Im, S.-S. *Langmuir* **2000**, *16*, 5841. (b) Kim, D.; Choi, J.; Kim, J.-Y.; Han, Y.-K. *Macromolecules* **2002**, *35*, 5314.
- (6) Wang, Z.; Heising, J. M.; Clearfield, A. *J. Am. Chem. Soc.* **2003**, *34*, 10375.

- (7) (a) Cheetham, A. K.; férey, G.; Loiseau, T. *Angew. Chem., Int. Ed.* **1999**, *38*, 3628. (b) Clearfield, A. *Chem. Mater.* **1998**, *10*, 2801. (c) Dines, M. B.; DiGiacomo, P. M. *Inorg. Chem.* **1981**, *20*, 92.
- (8) (a) Chan, H. B. S.; Budd, P. M.; Naylor, T. V. *J. Mater. Chem.* **2001**, *12*, 2068. (b) Lin, H. P.; Mou, C. Y.; Lin, S. B. *Adv. Mater.* **2000**, *12*, 103. (c) Gong, X.; Liu, J.; Baskaran, S.; Voise, R. D.; Young, J. S. *Chem. Mater.* **2000**, *12*, 1049. (d) Chen, C. C.; Chao, C. Y.; Lang, Z. H. *Chem. Mater.* **2000**, *12*, 1516.
- (9) (a) Cao, M.; Hu, C.; Wang, Y.; Guo, Y.; Guo, C.; Wang, E. *Chem. Commun.* **2003**, 1884. (b) Puentes, V. F.; Zanchet, D.; Erdonmez, C. K.; Alivisatos, A. P. *J. Am. Chem. Soc.* **2002**, *124*, 12874. (c) Li, Y. D.; Li, X. L.; Deng, Z. X.; Zhou, B.; Fan, S.; Wang, J.; Sun, X. *Angew. Chem., Int. Ed.* **2002**, *41*, 333.
- (10) Culp, J.; Fanucci, G.; Watson, B.; Morgan, A. N.; Backov, R.; Ohnuki, H.; Meisel, M.; Talham, D. *J. Solid State Chem.* **2001**, *159*, 362.
- (11) (a) Zhu, Y.-C.; Bando, Y.; Xue, D.-F.; Golberg, D. *Adv. Mater.* **2004**, *16*, 831. (b) Bonchio, M.; Carraro, M.; Scorrano, G.; Bagno, A. *Adv. Synth. Catal.* **2004**, *346*, 648. (c) Johnson, C. J.; Edler, K. J.; Mann, S.; Murphy, C. J. *J. Mater. Chem.* **2002**, 2909.

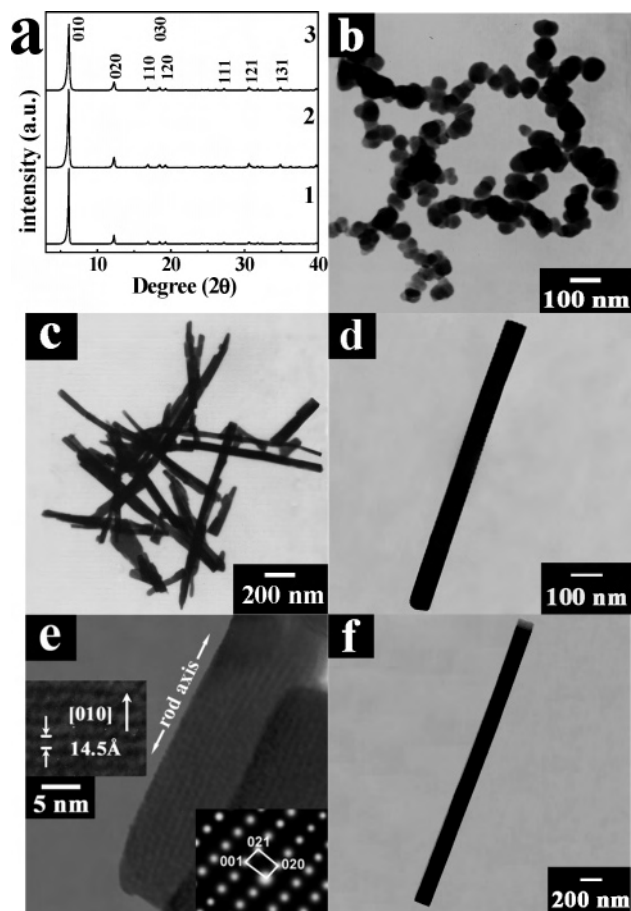
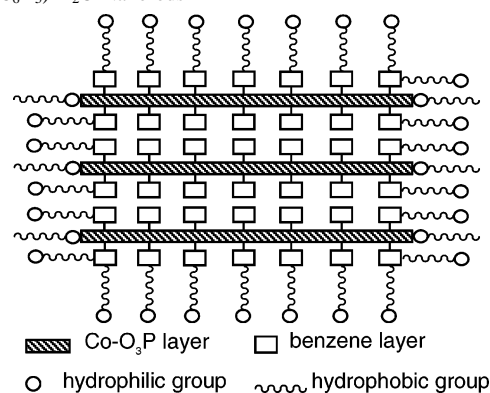


Figure 1. (a) XRD patterns of samples 1–3. (b) TEM image of sample 1. (c,d) TEM images of sample 2, (e) HRTEM image of sample 2 and (inset) SAED image. (f) TEM image of sample 3.

to be significant. In this work, we intended to prepare $\text{Co}(\text{O}_3\text{PC}_6\text{H}_5)\cdot\text{H}_2\text{O}$ nanoparticles and nanorods by the use of hydrothermal method. The reaction of $\text{Co}(\text{NO}_3)_2\cdot 6\text{H}_2\text{O}$ with sodium phenylphosphonate (SPP) in a 1:1 stoichiometry in water was carried out in a Teflon-lined autoclave at 100 °C for 2 days, and $\text{Co}(\text{O}_3\text{PC}_6\text{H}_5)\cdot\text{H}_2\text{O}$ nanoparticles were obtained. When the surfactants CTAB or SDBS were added into the reaction mixture, $\text{Co}(\text{O}_3\text{PC}_6\text{H}_5)\cdot\text{H}_2\text{O}$ nanorods formed.

X-ray powder diffraction (XRD) patterns of the samples were collected on a Rigaku D_{max} 2000 X-ray diffractometer with $\text{Cu K}\alpha$ radiation ($\lambda = 0.154178$ nm), with 2θ ranging from 2° to 40°. Sample 1 (nanoparticles) was prepared without use of surfactant, whereas samples 2 and 3 (nanorods) were prepared using CTAB and SDBS, respectively. The details of the syntheses are given in the Supporting Information. Figure 1a shows the XRD patterns of the three samples. All of the peaks of the three samples are to be the same and can be indexed to the simulated XRD powder pattern of $\text{Co}(\text{O}_3\text{PC}_6\text{H}_5)\cdot\text{H}_2\text{O}$ (Figure S10 in the Supporting Information), indicating that they are the same compound [$\text{Co}(\text{O}_3\text{PC}_6\text{H}_5)\cdot\text{H}_2\text{O}$]. The morphology of the prepared $\text{Co}(\text{O}_3\text{PC}_6\text{H}_5)\cdot\text{H}_2\text{O}$ was further investigated with transmission electron microscopy (TEM). Typical TEM images show that sample 1 is a particle-like shape with a diameter of 40–60 nm (Figure 1b) and samples 2 and 3 display straight, rod-like

Chart 1. Effect of Surfactant on the Growth Process of $\text{Co}(\text{O}_3\text{PC}_6\text{H}_5)\cdot\text{H}_2\text{O}$ Nanorods



shapes (Figure 1c, 1d, and 1f). A high-resolution TEM (HRTEM) image and selected area electron diffraction (SAED) pattern of the sample 2 (inset in Figure 1e), taken from a single rod, show that the nanorod is structurally uniform with a clearly resolved interplanar spacing of about 14.5 Å, which corresponds to (010) planes, and that the axis of the nanorod is along the [001] direction.

The hydrothermal synthesis method and the temperature have significant effects on the size and morphology of $\text{Co}(\text{O}_3\text{PC}_6\text{H}_5)\cdot\text{H}_2\text{O}$. When the reaction was carried out by stirring the mixture at 60 °C for 3 days, only bulk $\text{Co}(\text{O}_3\text{PC}_6\text{H}_5)\cdot\text{H}_2\text{O}$ was observed. When CTAB or SDBS was used in the reaction, $\text{Co}(\text{O}_3\text{PC}_6\text{H}_5)\cdot\text{H}_2\text{O}$ nanorods were obtained instead of nanoparticles. Clearly, the interaction between the surfactant and the reactant has a great effect on the result. Chart 1 illustrates the effect of surfactant on the growth process of $\text{Co}(\text{O}_3\text{PC}_6\text{H}_5)\cdot\text{H}_2\text{O}$ nanorods. $\text{Co}(\text{O}_3\text{PC}_6\text{H}_5)\cdot\text{H}_2\text{O}$ exhibits a lamellar structure with alternating $\text{Co}-\text{O}_3\text{P}$ and phenyl layers. The hydrophobic groups of CTAB connect to the top and bottom phenyl layers of $\text{Co}(\text{O}_3\text{PC}_6\text{H}_5)\cdot\text{H}_2\text{O}$ with van der Waals forces, which can efficiently prevent the particle from growing along the direction perpendicular to the layers. However, in the side of the lamellar structure, the hydrophilic $\text{Co}-\text{O}_3\text{P}$ layer and hydrophobic phenyl layer stack alternately, so no stable protecting shell of CTAB can be formed. The growth of $\text{Co}(\text{O}_3\text{PC}_6\text{H}_5)\cdot\text{H}_2\text{O}$ nanorods along the c axis rather than the a axis can be determined by its highly anisotropic character along the c axis. The structure of the inorganic polymeric $\text{Co}-\text{O}_3\text{P}$ layer is shown in Figure 2.¹² Each cobalt ion is coordinated to five phosphonate oxygen atoms and one water molecule. Each phosphonate group is coordinated to four cobalt ions. The two-dimensional polymeric structure can be described as columns built up of alternating cobalt and phosphonate ions, extending along the c axis, with each column is linked to two neighboring columns. Thus, the anisotropic character along the c axis is apparently different from that along the a axis. From a kinetic perspective, the activation energy for the [001] direction of growth of $\text{Co}(\text{O}_3\text{PC}_6\text{H}_5)\cdot\text{H}_2\text{O}$ is lower than that for growth

- (12) (a) Cunningham, D.; Hennelly, P. J. D.; Deeney, T. *Inorg. Chim. Acta.* **1979**, *37*, 95. (b) Zhang, Y. P.; Clearfield, A. *Inorg. Chem.* **1992**, *31*, 2821. (c) Cao, G.; Lee, H.; Lynch, V. M.; Mallouk, T. E. *Inorg. Chem.* **1988**, *27*, 2781. (d) Cao, G.; Lee, H.; Lynch, V. M.; Mallouk, T. E. *Solid State Ionics* **1988**, *26*, 63.

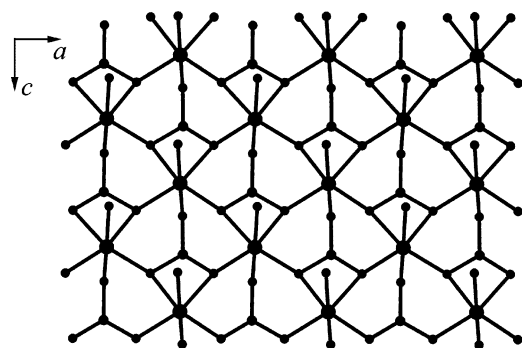


Figure 2. Structure of an inorganic polymeric layer of $\text{Co}(\text{O}_3\text{PC}_6\text{H}_5)\cdot\text{H}_2\text{O}$.

along the a axis. This means a higher growth rate along the c axis and a lower one along the a axis to form $\text{Co}(\text{O}_3\text{PC}_6\text{H}_5)\cdot\text{H}_2\text{O}$ nanorods that grow preferentially along the $[001]$ direction.¹³ Different concentration ratios of $[\text{CTAB}]/[\text{SPP}]$ gave nanorods with different diameters: 30–40 nm ($[\text{SPP}] = 5$ mM, $[\text{CTAB}] = 40$ mM), 50–60 nm ($[\text{SPP}] = 20$ mM, $[\text{CTAB}] = 40$ mM), and 70–80 nm ($[\text{SPP}] = 40$ mM, $[\text{CTAB}] = 40$ mM). With a high concentration ratio of $[\text{CTAB}]$ to $[\text{SPP}]$, the surfactant can envelop the crystal seeds of $\text{Co}(\text{O}_3\text{PC}_6\text{H}_5)\cdot\text{H}_2\text{O}$ well, which leads to the formation of nanorods with small diameters.

Divalent metal phenylphosphonates $\text{M}(\text{O}_3\text{PC}_6\text{H}_5)\cdot\text{H}_2\text{O}$ ($\text{M} = \text{Mn}, \text{Ni}, \text{Cu}, \text{Zn}, \text{Cd}$) also have lamellar structures.¹² When $\text{Ni}(\text{NO}_3)_2\cdot 6\text{H}_2\text{O}$ was used instead of $\text{Co}(\text{NO}_3)_2\cdot 6\text{H}_2\text{O}$, nanoparticles and nanorods of $\text{Ni}(\text{O}_3\text{PC}_6\text{H}_5)\cdot\text{H}_2\text{O}$ could be prepared analogously. However when $\text{M}(\text{NO}_3)_2\cdot 6\text{H}_2\text{O}$ ($\text{M} = \text{Mn}, \text{Cu}, \text{Zn}, \text{Cd}$) was used, only nanoparticles of $\text{M}(\text{O}_3\text{PC}_6\text{H}_5)\cdot\text{H}_2\text{O}$ ($\text{M} = \text{Mn}, \text{Cu}, \text{Zn}, \text{Cd}$) were obtained even if surfactant (CTAB or SDBS) was used. The probable reason is that the van der Waals force between the adjacent phenyl layers is much stronger than those between the phenyl layer and the hydrophobic groups of CTAB so that the surfactant cannot change the morphology of the metal phenylphosphonate.

Heating the nanorods at 600 °C in air for 2 h yielded bluish-violet nanoporous crystalline $\text{Co}_2\text{P}_2\text{O}_7$ without altering the 1D morphology, and many holes formed in the nanorods (Figure 3b). From TGA analysis (see Supporting Information), a total of 37.4% weight loss was observed from 200

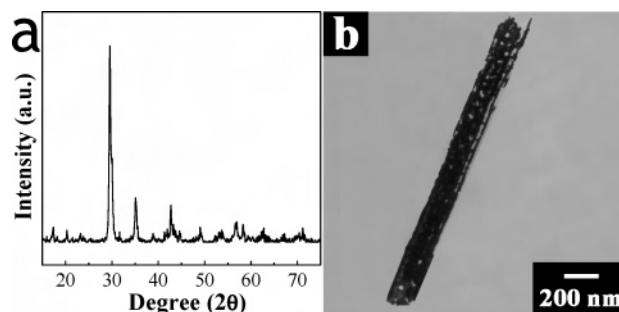


Figure 3. XRD pattern and TEM image of sample 2 after heating.

to 600 °C under N_2 , which is consistent with the calculated value of 37.4% considering the loss of the organic portion. The holes in crystalline $\text{Co}_2\text{P}_2\text{O}_7$ are formed by removing the organic part of the $\text{Co}(\text{O}_3\text{PC}_6\text{H}_5)\cdot\text{H}_2\text{O}$. All of the diffraction peaks in the XRD pattern of the sample after heating (Figure 3a) can be indexed to pure monoclinic $\text{Co}_2\text{P}_2\text{O}_7$ [space group $P2_1/c$] with lattice constants $a = 7.008$ Å, $b = 8.345$ Å, and $c = 9.004$ Å (JCPDS 79-0825). Element analysis obtained via inductively coupled plasma-atomic emission spectrometry (ICP-AES) (Labtest Equipment Co. model 710) further confirms the elemental composition of the compounds in the expected stoichiometric proportions, obsd (%) Co, 41.02; P, 20.84; calcd (%) Co, 40.39, P, 21.23.

In summary, a surfactant-directed synthetic route was developed for the synthesis of metal phosphonate nanostructures. The unique properties combined with the simple and controllable synthetic approach can provide useful information for the study in related fields.

Acknowledgment. We thank the National Natural Science Foundation of China (No. 20471014) and the Fok Ying Tung Education Foundation for support. TEM work was performed by Doctor L.-H. Ge at the Changchun Institute of Applied Chemistry, Chinese Academy of Sciences, Changchun, China.

Supporting Information Available: Experiment section. Thermal gravimetric curve for sample 2 (Figure S1). Images of the samples obtained using different concentration ratios of $[\text{CTAB}]$ to $[\text{SPP}]$ (Figures S2 and S3). TEM images of other transition metal phosphonates (Figures S4–S9). Simulated XRD powder pattern of $\text{Co}(\text{O}_3\text{PC}_6\text{H}_5)\cdot\text{H}_2\text{O}$ (Figure S10). This material is available free of charge via the Internet at <http://pubs.acs.org>.

IC048436T

(13) Fang, Y.-P.; Xu, A.-W.; Song, R.-Q.; Zhang, H.-X.; You, L.-P.; Yu, J. C.; Liu, H.-Q. *J. Am. Chem. Soc.* **2003**, *125*, 16025.